

University of Texas at Arlington

**MavMatrix**

---

2019 Spring Honors Capstone Projects

Honors College

---

5-1-2019

## **CALIBRATION OF CANTILEVER BEAM LOAD CELLS FOR DETECTING PRESSURE AND SHEAR IN PROSTHETIC SOCKET APPLICATIONS**

Elida Sorto-Ramos

Follow this and additional works at: [https://mavmatrix.uta.edu/honors\\_spring2019](https://mavmatrix.uta.edu/honors_spring2019)

---

### **Recommended Citation**

Sorto-Ramos, Elida, "CALIBRATION OF CANTILEVER BEAM LOAD CELLS FOR DETECTING PRESSURE AND SHEAR IN PROSTHETIC SOCKET APPLICATIONS" (2019). *2019 Spring Honors Capstone Projects*. 24. [https://mavmatrix.uta.edu/honors\\_spring2019/24](https://mavmatrix.uta.edu/honors_spring2019/24)

This Honors Thesis is brought to you for free and open access by the Honors College at MavMatrix. It has been accepted for inclusion in 2019 Spring Honors Capstone Projects by an authorized administrator of MavMatrix. For more information, please contact [leah.mccurdy@uta.edu](mailto:leah.mccurdy@uta.edu), [erica.rousseau@uta.edu](mailto:erica.rousseau@uta.edu), [vanessa.garrett@uta.edu](mailto:vanessa.garrett@uta.edu).

Copyright © by Elida Sorto-Ramos 2019

All Rights Reserved

CALIBRATION OF CANTILEVER BEAM LOAD CELLS FOR  
DETECTING PRESSURE AND SHEAR IN  
PROSTHETIC SOCKET  
APPLICATIONS

by

ELIDA SORTO-RAMOS

Presented to the Faculty of the Honors College of  
The University of Texas at Arlington in Partial Fulfillment  
of the Requirements  
for the Degree of

HONORS BACHELOR OF SCIENCE IN AEROSPACE ENGINEERING

THE UNIVERSITY OF TEXAS AT ARLINGTON

May 2019

## ACKNOWLEDGMENTS

Firstly, I would like to thank my supervising professor, Dr. Haiying Huang, for her endless support and encouragement and for always challenging me throughout my undergraduate career.

Furthermore, I am grateful for my family who have always supported my ambitious goals and dreams. Thank you for allowing me to flourish. I am thankful I had a loving and nurturing upbringing by my late mother without whom I would not be where I am today.

Lastly, I would like thank God who has given me this amazing, wonderful, and thoughtful life. I am humbled by the greatness of His wonders and what the future has in store.

May 09, 2019

## ABSTRACT

# CALIBRATION OF CANTILEVER BEAM LOAD CELLS FOR DETECTING PRESSURE AND SHEAR IN PROSTHETIC SOCKET APPLICATIONS

Elida Sorto-Ramos, B. S. Aerospace Engineering

The University of Texas at Arlington, 2019

Faculty Mentor: Dr. Haiying Huang

In this paper the pressure and shear forces are quantified at the interface of a prosthetic socket and the residual limb. This is useful in determining the amount of adjustment needed during the prosthetic fitting procedure. The correct fit of the prosthesis is essential for complete and timely rehabilitation of the patient and return to normal ambulation after amputation. A cantilever beam load cell was developed to measure strain and inversely determine the pressure that caused it. The measurement system was verified with theoretical calculations and computational analysis. The results produced a cantilever beam load cell that can calibrate an antenna patch sensor for noninvasive measurement of

interfacial stresses at the prosthetic socket-residual limb interface. The cantilever beam load cell predicted the pressure induced on it within one percent of the actual value.

## TABLE OF CONTENTS

ACKNOWLEDGMENTS .....	iii
ABSTRACT.....	iv
LIST OF ILLUSTRATIONS .....	vii
LIST OF TABLES .....	viii
Chapter	
1. INTRODUCTION .....	1
2. LITERATURE REVIEW .....	3
3. METHODOLOGY .....	6
4. RESULTS AND DISCUSSION.....	9
4.1 Finite Element Analysis.....	9
4.2 Validation of Strain Measurement System .....	11
4.3 Calibration of Cantilever Beam Load Cell .....	13
4.4 Inverse Algorithm .....	15
5. CONCLUSION.....	19
6. FUTURE WORK.....	20
REFERENCES .....	21
BIOGRAPHICAL INFORMATION.....	25

## LIST OF ILLUSTRATIONS

Figure	Page
3.1 Schematic of Cantilever Beam Load Cell .....	7
3.2 Geometry of CBLC .....	8
4.1 Finite Element Model .....	10
4.2 Strain Measurement System Calibration .....	12
4.3 Test Specimen Mounted into Tensile Machine .....	12
4.4 Laboratory Setup .....	14
4.5 Measured Strains and their Average .....	15
4.6 Average Measured Strain Compared to Theory .....	15



## LIST OF TABLES

Table	Page
3.1 Properties of Cantilever Beam.....	6
4.1 Results of FEA .....	11
4.2 Validation of Inverse Algorithm .....	16
4.3 Pressure Results from MATLAB code with corrected Young's Modulus.....	17

## CHAPTER 1

### INTRODUCTION

Technology has enabled humans to achieve remarkable feats that had not been possible previously. Long ago, the loss of a lower-limb meant the loss of the ability to ever walk again. Today, technology has advanced to enable people to walk, dance, and climb even better than they had before. Amputations affect approximately one in 190 Americans today (Ziegler-Graham et al.) and the figures only go up for people worldwide. The main causes of amputations are vascular diseases and trauma (Ziegler-Graham et al.). Often times amputees look forward to obtaining a prosthesis because it allows them to regain their mobility and lessens the effect of having lost a limb. However, obtaining the proper fitting prosthesis is hardly a straightforward procedure. Patients must frequently return to clinics to have their prosthesis modified for a better fit. This is tedious, painful and an ineffective way to provide a medical service. Prosthetic fitting procedures need to be improved to allow for a quick rehabilitation and return to normal mobilization. Return to an active lifestyle as soon as possible can help reduce future health complications for the patient (Pohjolainen, Alaranta, & Wikstrom, 1989).

Despite the advances in medical technology, current fitting procedures are limited to conventional socket casting and Computer Aided Socket design (Sewell, Noroozi, Vinney, & Andrews, 2000). Computer aided socket design uses noninvasive measurements of the residual limb to form the model and fabricate the socket, which leaves little room for the prosthetist to make adjustments (Sewell, Noroozi, Vinney, & Andrews, 2000).

However, these methods are not able to accurately predict the interfacial stresses. In order to better understand the delicate interaction between the residual limb and the prosthetic socket it is important to know the force distribution present. The purpose of this study is to investigate the forces experienced by a prosthetic user at the limb-socket interface. The two main forces that develop at the interface are pressure and shear; pressure is the force acting perpendicular to a surface while shear is the force acting parallel. The pressure and shear distribution may lead to areas of stress concentration at the interface which causes negative effects on the skin. As these forces exceed the skins' pain threshold, they cause discomfort which results in skin irritation and the formation of ulcers, cysts, blisters and even breaking of the skin (Sanders, 1996). Acceptable amounts of these forces have not yet been quantified in the laboratory.

In this study, a calibration procedure will be established for sensors that will be able to measure the forces occurring at the interface of the prosthetic socket and a residual limb. By better understanding the forces that act on the surface, a prosthetic socket can be fabricated with greater accuracy and knowledge as to the regions of stress concentration and necessary modifications can be made during the socket fitting procedure.

## CHAPTER 2

### LITERATURE REVIEW

Various models exist that determine the shear and pressure forces at an interface. Sensors include strain gages, piezoelectrical resistors, and capacitance-based measurements (Agcayazi et al). T. Agcayazi, M. McKnight, P. Sotory, H. Huang, T. Ghosh, and A. Bozkurt have developed a sensor that uses the change in capacitance as a function of shear force on the surface. Their setup employs an array of sensors placed between the prosthetic socket and the socket liner. Capacitance measures the amount of charge that can be stored between two charged plates and is related to the area of the plates, the distance between them and a dielectric constant. Agacayazi et al. have concluded that measurement with these sensors is accurate. Sources of error may include electromagnetic interference from external sources such as the human body which acts as a stray capacitor. This method provided a wireless, nonintrusive measurement of the forces at the interface. They were able to overcome the challenges of integrating a flexible sensor with a mechanically stable prosthetic socket by making the array of a flexible copper and connecting it to a flexible mesh. However, they have not been able to identify the shear force on the surface, only the change in force intensity.

Another sensor element is a strain gage. Strain gages rely on the changing resistance of the material once placed under stress. The governing equation for strain gages is as follows:

$$\Delta R = R \varepsilon GF \quad (1)$$

where  $\Delta R$  is the change in resistance,  $R$  is the resistance of the strain gage,  $\varepsilon$  is the strain and  $GF$  is a gauge factor characteristic of the strain gage (Al-Fakih, 2016). They are widely accepted because they are manufactured and distributed at a low cost and have a wide sensing range and good sensitivity (Mohsin, 2012). The sensors must be bonded to the surface of measurement therefore these types of sensors are usually mounted to the socket wall or an external sensing device (Al-Fakih, 2016). Strain gages are connected to a Wheatstone bridge circuit to capture the change in resistance.

Various methods of installing the sensors have also been tested (Sanders 1995). J.E. Sanders and C.H. Daly have reported three main methods of stress measurement. These include: i) inserting a thin pressure sensor between the skin and the socket, ii) installing the transducers through a hole cut in the socket wall and iii) separating a section of the wall for measurement on that specific area (Sanders, 1993). By inserting sensors between the skin and the socket, stress concentrations in the edges of the sensor are produced which alter the measurement (Sanders 1995). By installing the transducers through a hole cut in the socket wall, edge stress concentrations are reduced, however the transducers were very large and added considerable weight to the system (Sanders 1993). Sensors positioned within the socket wall and isolated from the rest of the residual limb compromised the suction and normal operation of the socket, therefore invalidating the sensors for localized force measurement (Sanders 1993). The results of their experiment concluded that their

triaxial pressure transducers had high sensitivity error due to transducer protrusion of the socket. This further increases the need for a noninvasive sensor. Furthermore, they concluded that tissue response depends on the direction of loading.

Dumbleton et al. studied two different prosthetic casting processes in 2009. They developed two prosthetic sockets for a group of users. One was casted using a method that would create an ideal pressure distribution on the surface by measuring the thickness of the residual limb at various locations and adjusting the fit of the socket. The other socket was casted by conventional hand methods. Their results showed that the ideal pressure distribution socket recorded higher peak pressures, indicating the complexity of the soft tissue at question. However, the users of either socket never experienced discomfort. This study further increased the need for a measurement system of interface pressure.

Shear force is very difficult to measure. In a study conducted by Mortimer et al. they measured in-shoe pressure and shear force with inductive coupling between a small target and adjacent coils. With this method they were able to measure the lateral displacement of the target and calculate the shear force that way. Problems with these types of sensors is the difficulty in measuring a displacement without slip and the cross-coupling between pressure and shear measurement. They recognize that measuring shear is an indicator of various steps in the gait cycle and can be a predictor of balance instability in the user. Therefore, increasing the need for an interface shear sensor.

## CHAPTER 3

### METHODOLOGY

In this study, a cantilever beam load cell sensor was developed to measure shear and pressure acting on a body. The cantilever beam load cell (CBLC) was designed as a machined rectangular bar with a slotted hole in the center. This would allow it to have a thin cross-section at the location of strain measurement while maintaining its stiffness to not buckle under the operative loading. The dimensions of the beam are reported in Table 3.1 and a model is shown in Figure 3.1. The CBLCs were manufactured from Aluminum 2024 in the Mechanical and Aerospace Engineering Machine Shop in Woolf Hall. A block was fixed to the end of the CBLC to allow for pressure to be applied at different offset distances in the laboratory.

Table 3.1: Properties of Cantilever Beam

Dimension	Value
Y, mm	6
S, mm	12
t, mm	1
A, mm <sup>2</sup>	24
I, mm <sup>4</sup>	728

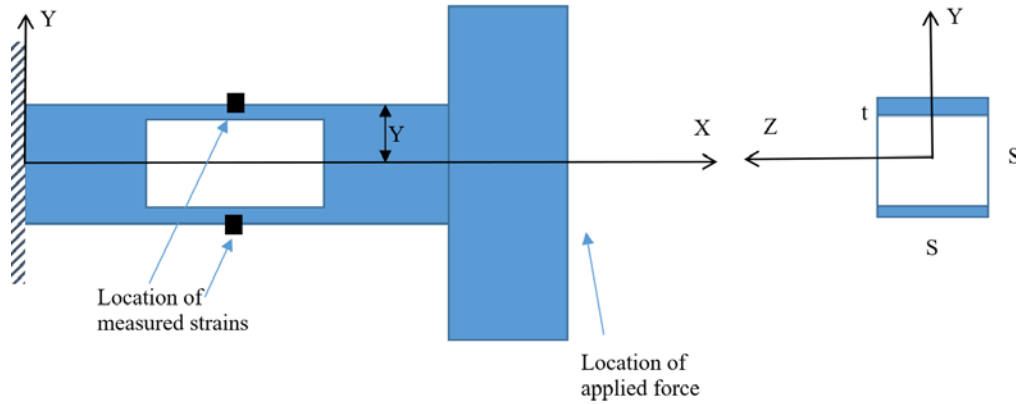


Figure 3.1: Schematic of Cantilever Beam Load Cell

Strain gages were installed onto the surface to measure the strain generated once a pressure or shear force was applied. The strain gages were installed using a bonding adhesive. The elongation of the strain gages, once loaded, was transduced to a change in resistance and captured as a voltage measured by an Arduino board for data collection. The Arduino was able to accurately output the strains due to a calibration procedure conducted with a National Instruments strain detector. The expected strains were calculated using Equations 2-5 from Gere, 2018. In these equations  $\sigma$  indicates the normal stress or stress perpendicular to the measurement surface. There are two forces that contribute to the normal stress, pressure (P) and shear (V).

$$\sigma_N = \frac{P}{A} \quad (2)$$

$$\sigma_M = \frac{V L_v Y}{I} \quad (3)$$

$$\sigma = \sigma_N + \sigma_M \quad (4)$$

$$\sigma = E\varepsilon \quad (5)$$

In these equations  $L_v$  is the distance between the measurement location and the location of applied shear, A is the cross-sectional area, I is the area-moment of inertia and



Y is the vertical distance from the neutral axis to the strain location measurement, as shown in Fig. 3.2.

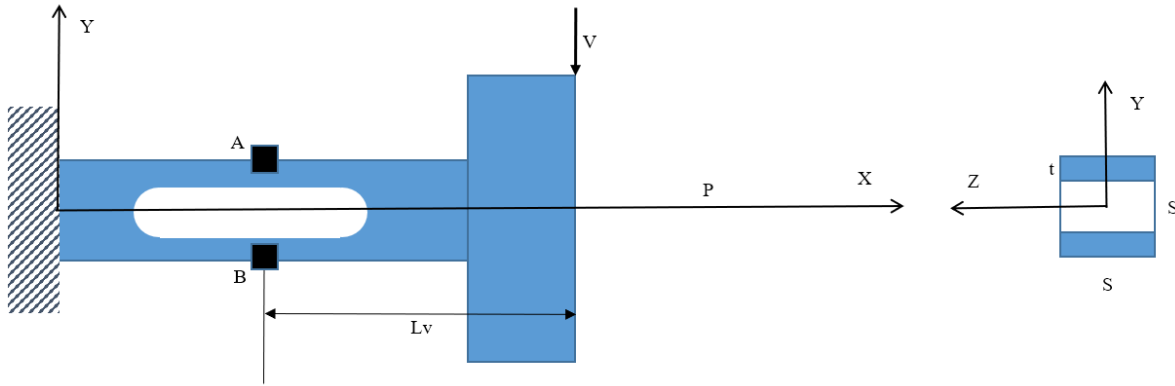


Figure 3.2: Geometry of CBLC

Since Y is positive for one strain gage and negative for the other, the normal stress due to bending moment will be added at one location and subtracted at the other. Once the stress is determined from the pressure and shear force, the strain at that location is known from Hooke's law (Eqn. 5). The theoretical calculations were verified with a computational finite-element solver. Furthermore, the measured values were compared to both the theoretical and computational results.

## CHAPTER 4

### RESULTS AND DISCUSSION

#### 4.1 Finite Element Analysis

Finite element analysis is conducted by representing the physical structure with a finite number of simple elements known as a mesh over which a mathematical model will be solved. In order to solve the governing differential equations, boundary conditions must first be specified. In this manner the complex continuous problems can be discretized and solved for numerically. The finite element analysis (FEA) software used in this project was ANSYS. The purpose of this procedure is to ensure the physical behavior of the system will be as predicted by theory. The Static Structural test was run after the geometry of the cantilever beam load cell was modelled in SolidWorks. A fine mesh was used to obtain an adequate resolution of the solution. The mesh was optimized at the size such that the output solution would no longer change. A known pressure and shear force were applied to the sensor and the strains were measured. The probe feature was used to estimate the value of strain at the location of strain gage measurement. The mesh used is shown Figure 4.a. In the computational model the boundary conditions of the model were specified as follows: one end of the cantilever beam was held fixed while a point load was placed on the other; this simulated the CBLC under compression.

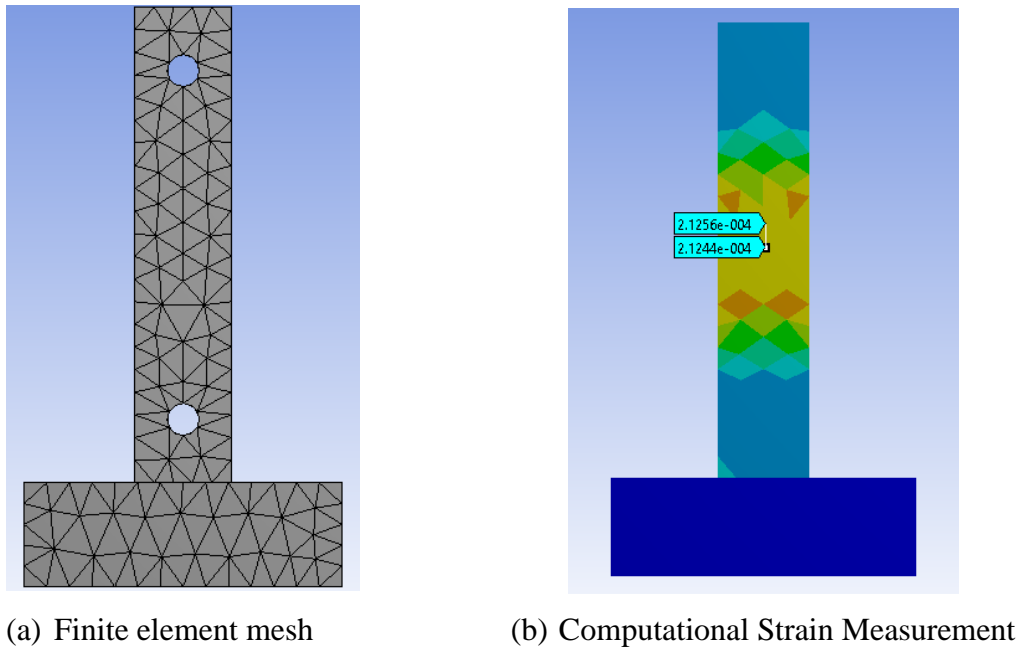


Figure 4.1: Finite Element Model

A comparison of the finite element model with the theoretical results was needed to verify the model. The material properties used in the ANSYS model were input from Aerospace Specification Metals Inc [2] with a Young's modulus of 73.1 GPa. The results of the finite element analysis are shown in. In this simulation a pressure force was applied at the neutral axis of the CBLC. This would produce normal stress as described by Eqn. 2. All the errors fell below 4% which is an acceptable value for the simulation.

Table 4.1: Results of FEA

Load (N)	Theory		FEA		Percent Error	
	SG1	SG2	SG1	SG2	SG1	SG2
0	0.0	0.0	0.00	0.00	0.00	0.00
50	27.4	27.4	26.55	26.57	-2.96	-2.90
100	54.7	54.7	53.58	52.87	-2.08	-3.37
150	82.1	82.1	80.37	79.31	-2.08	-3.37
200	109.4	109.4	106.22	106.27	-2.94	-2.90
250	136.8	136.8	132.48	132.65	-3.16	-3.03
300	164.2	164.2	158.98	159.18	-3.15	-3.03
350	191.5	191.5	187.53	185.06	-2.08	-3.37
400	218.9	218.9	212.44	212.56	-2.94	-2.89

Sources of error in the finite element model could be the input geometry, which is not always exact when fabricated. Error could also arise from the exact material properties that vary between different alloys of the same material. Also, finite element solvers solve complex polynomials over each element which produces a higher degree of accuracy than the general equations for uniform cross sections. Once the finite element model was verified, the strains could be measured physically in the laboratory and compared to the exact solution.

#### 4.2 Validation of Strain Measurement System

The strain measurement system, National Instruments Data Acquisition System (NI DAQ), was validated experimentally to ensure proper operation. The validation of the measurement system was completed using a dog-bone specimen made of Aluminum 6061 and a Shimadzu Material Testing System (MTS). A strain gage was installed onto the surface of the specimen and the strains were measured with the NI DAQ. The specimen was fixed onto the MTS as shown in Figure 4.3. The specimen was then loaded in tension up to 10 kN or 3400 microstrain. The results of the experiment were compared to the

theoretical values calculated with Eqn. 2 in Figure . The curve-fit equations for the theoretical values calculated with Eqn. 2 in Figure 4.2. The curve fit equations for the theoretical and experimental results agreed within 2.44%. This validated the measurement system and proved it was reading the correct value of strain.

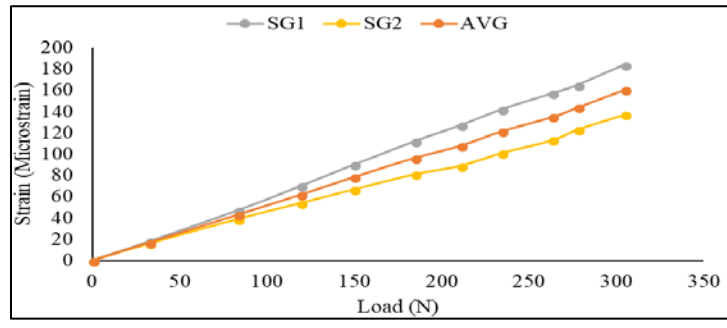


Figure 4.2: Strain Measurement System Calibration

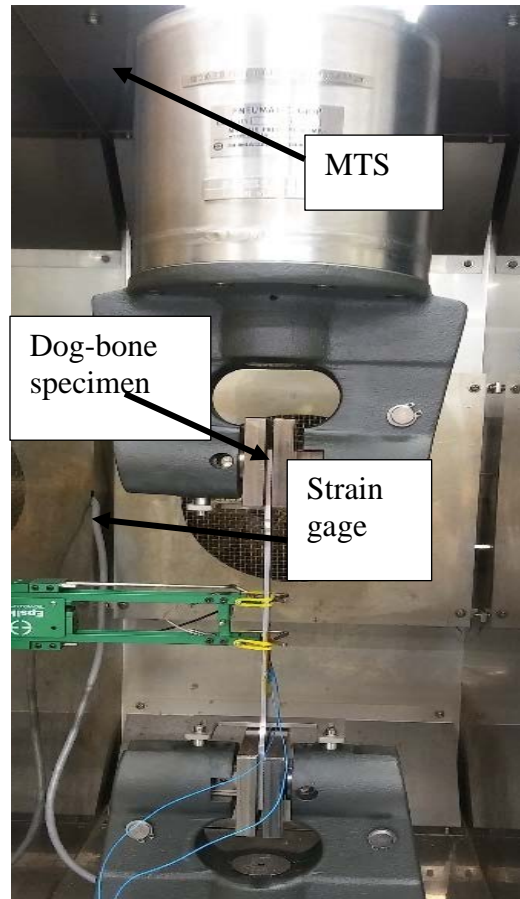


Figure 4.3: Test Specimen Mounted into Tensile Machine

### 4.3 Calibration of Cantilever Beam Load Cell

Subsequently the strain gages mounted on the cantilever beam load cell were calibrated. This was completed using a laboratory setup shown in Figure 4.4. The laboratory setup consisted of the CBLC mounted to a test fixture. A pressure block was placed on top of a load cell. The pressure block would apply pressure evenly to the CBLC and the load cell would measure the amount of applied pressure through the Arduino board. Both the load cell and pressure block were set on a linear motor. The linear motor was controlled by the Arduino microcontroller. The tests conducted with this setup isolated the applied pressure. This meant that the strains developed would only be a result of Eq. 2. Measurement of strain were taken with the NI DAQ. Pressure was applied from 0 to 300 newtons which produced strain in the range of 0 to 170 microstrain. This operating range was chosen because the sensors measured interfacial stress.

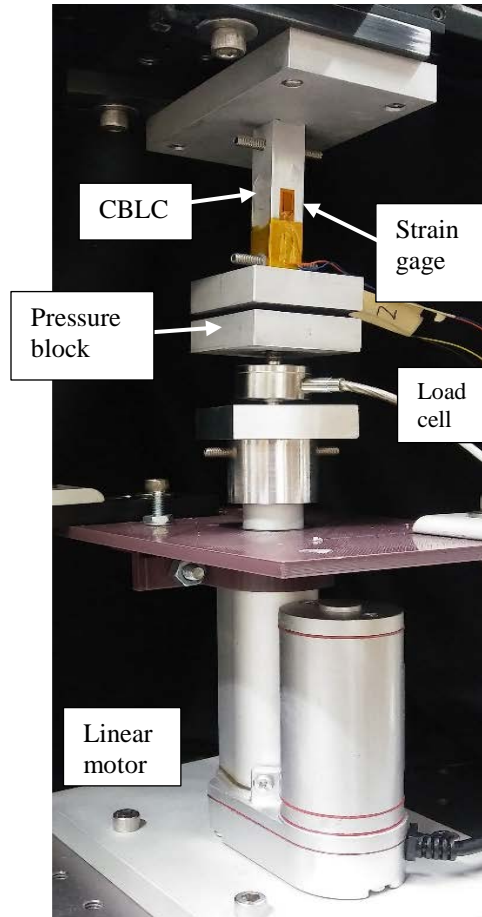


Figure 4.4: Laboratory Setup

The measurement from each strain gage and the average of the two measurements was plotted as shown in Figure 5. The average of the strains was compared to theory and the result matched the theoretical prediction within 6.94% as shown in Figure 4.6. The average was taken because it quantified the normal stress due to pressure force as will be seen in Eq. 6. This value error was accepted.

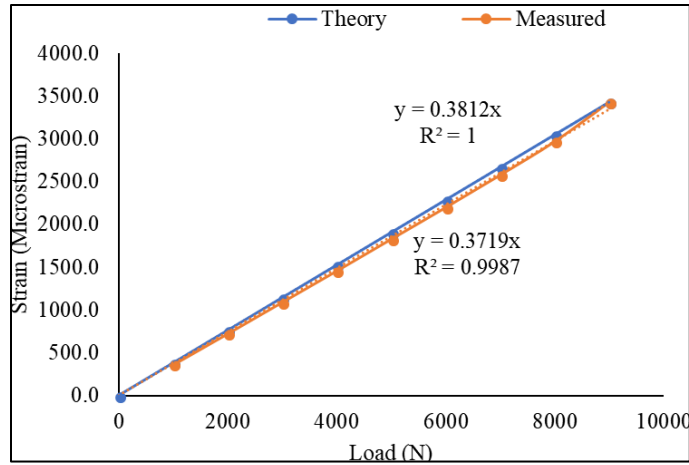


Figure 4.5: Measured Strains and their Average

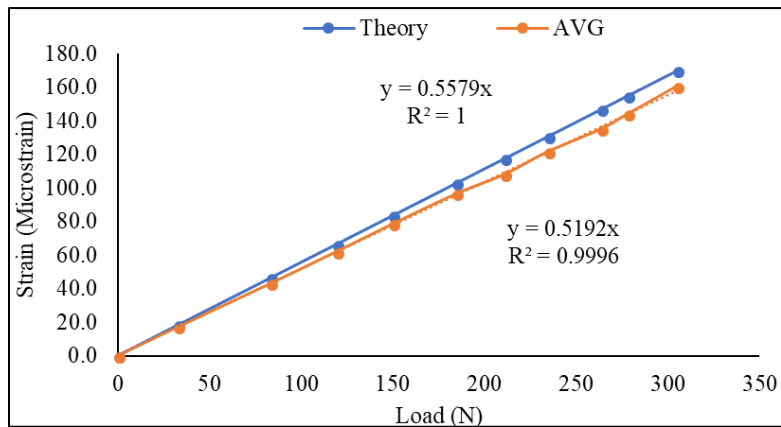


Figure 4.6: Average Measured Strain Compared to Theory

#### 4.4 Inverse Algorithm

Once verified, the strain gages could predict the pressure from their measured values using an inverse calculation. The inverse calculation was implemented into a MATLAB program. The inverse calculations solve the following set of equations from the measured strains. In these equations and are the stresses measured indirectly by the strain gages. The average of the two values (Eq. 6) is characteristic of the normal stress due to pressure force acting on the sensor. Half of the difference of these two measurements are



a direct indication of the bending stress acting on the sensor (Eq. 7) and therefore output the shear force.

$$\sigma_N = \frac{\sigma_A + \sigma_B}{2} \quad (6)$$

$$\sigma_M = \frac{\sigma_A - \sigma_B}{-2} \quad (7)$$

Verification of the inverse algorithm was completed with a simulated set of strains. Shear force can be modelled as pressure applied at an offset distance from the neutral axis to produce a bending moment stress. The bending moment stress would put one side of the CBLC in compression and the other in tension. This would be reflected in different values of strain measured at both sides of the CBLC. The simulated strains were calculated from the theoretical equations with a pre-determined pressure and offset distance. The strains were then fed into the MATLAB code and the output was tabulated in Table 4.. The error between the applied force and distance offset all fell on the order of magnitude of 10E-14. This exponentially small value was approximated as zero and the inverse algorithm was accepted for future use.

Table 4.2: Validation of Inverse Algorithm

Input				Output		Error in Output	
Pressure (N)	Distance (m)	$\mu\epsilon$ at A	$\mu\epsilon$ at B	Pressure (N)	Distance (m)	Pressure	Distance
50.0	0.0130	43.9	-99.7	50.00	0.0130	1.42E-14	2.67E-14
100.0	0.0120	76.8	-188.4	100.00	0.0120	1.42E-14	1.45E-14
150.0	0.0110	98.7	-266.0	150.00	0.0110	1.89E-14	1.58E-14
200.0	0.0100	109.5	-332.6	200.00	0.0100	1.42E-14	1.73E-14
250.0	0.0090	109.2	-388.1	250.00	0.0090	2.27E-14	1.93E-14
300.0	0.0080	97.9	-432.6	300.00	0.0080	1.89E-14	0.00E+00
350.0	0.0070	75.5	-466.0	350.00	0.0070	1.62E-14	2.48E-14
400.0	0.0060	42.1	-488.4	400.00	0.0060	4.26E-14	1.45E-14
450.0	0.0050	-2.4	-499.7	450.00	0.0050	1.26E-14	1.73E-14
500.0	0.0040	-57.9	-500.0	500.00	0.0040	2.27E-14	0.00E+00

In order to obtain more accurate experimental results, the Young's modulus of the CBLCs was determined experimentally. This was done by plotting the sum of the strains versus the pressure applied. The sum of the strains would yield the following equation:

$$\epsilon_A + \epsilon_B = \frac{2P}{AE} \quad (8)$$

A linear curve fit to this data set would give a constant slope of  $2/AE$ . Since the area is known, the actual modulus can be extracted. The experimental modulus was obtained to be 78.54 GPa, as compared to the theoretical modulus of 73.1 GPa. This is an error of 7.44% which matches the offset between the theoretical value of strain and the average of the measured values. The results of the MATLAB code improved once the inverse calculation used Young's modulus obtained from the experimental data. The results are shown in Table4.3 and all fall around 1% error.

Table 4.3: Pressure Results from MATLAB Code with Corrected Young's Modulus

Actual (N)	Calculated (N)	Percent error
0	0	
32.5	32.7	0.8
83.2	82.8	0.4
119.2	119.4	0.2
149.9	151.2	0.9
184.6	185.8	0.7
210.8	208.0	1.4
234.4	234.0	0.2
263.3	260.0	1.3
278.0	277.3	0.2
304.7	309.1	1.4

## CHAPTER 5

### CONCLUSION

Pressure and shear sensors are vital for the advancement of medical technology and the creation of a proper prosthetic fitting procedure. This study produced a cantilever beam load cell that was sensitive to pressure. The strain gages mounted to the CBLC were able to accurately capture the physics of the problem. The inverse calculation predicted the pressure within 1% error. The sensors developed here would provide significant insight into the interfacial stresses and thus the proper prosthetic socket fitting procedure.

The results of this work produced an accurate algorithm for converting measured strains into shear and pressure values which aides in quantifying the sensitive areas experience at an interface. This is especially important in the preliminary design process of the prosthetic socket to ensure adequate fit throughout its lifetime.

## CHAPTER 6

### FUTURE WORK

The cantilever beams would then be used to calibrate the antenna sensors. Antenna sensors consist of a few main components, a nonconductive ground plate, a substrate, the sensor and a superstrate, if applied; stacked in that order. These sensors take the transmission of electromagnetic waves and convert it to a radiating signal (Balanis, 2016). The radiating signal resonates at a particular frequency dependent on the design of the sensor. Once loaded by a pressure or shear force, the physical properties of the patch antenna change in space, such as the thickness of the dielectric and the height from the ground plate. This causes a change in the electromagnetic signal being transmitted and therefore the radiation frequency. This change in frequency to the forces applied through calibration. The calibration procedure will determine the amount of pressure or shear present at a certain frequency output of the sensors. The pressure and shear will be known because of the strains measured on the cantilever beam and the inverse algorithm. The changing frequency with changing force has been quantified in a study by H. Huang et al. The results of the study will be used to predict the behavior of the antenna sensors. Antenna sensors are advantageous because they would be embedded into the socket liner. This allows for the direct measurement of interfacial stresses felt by the patient. Another advantage is that they will not produce stress concentrations and are not susceptible to movement.

## REFERENCES

1. Agcayazi T., McKnight M., Sotory P., Huang H., Ghosh T., Bozkurt A., "A scalable shear and normal force sensor for prosthetic sensing," 2017 IEEE SENSORS, Glasgow, 2017, pp. 1-3.
2. "Aluminum 2024-T4; 2024-T351." ASM Material Data Sheet. N.p., n.d. Web. 03 July 2018.
3. Al-Fakih, E.A., Osman A., Azuan N., Adikan M., Rafiq F., "Techniques for interface stress measurements within prosthetic sockets of transtibial amputees: A review of the past 50 years of research" Source: Sensors (Switzerland), v 16, n 7, July 20, 2016
4. Amali, R.; Noroozi, S.; Vinney, J.; Sewell, P.; Andrews, S. "Predicting interfacial loads between the prosthetic socket and the residual limb for below-knee amputees—A case study". Strain 2006, 42, 3–10.
5. Appoldt F.A.; Bennett L.; Contini R., "Tangential pressure measurements in above-knee suction sockets" Source: U S, Veterans Admin, Dep Med Surg, n 10-13, p 70-86, Spring 1970
6. Baars, E.; Geertzen, J., "Literature review of the possible advantages of silicon liner socket use in trans-tibial prostheses". Prosthet. Orthot. Int. 2005, 29, 27–37.
7. Balanis, Constantine A., "Antenna Theory: Analysis and Design". Hoboken, NJ: John Wiley & Sons, 2016. Print.

8. Chun-Te Chang, Chao Shih Liu, William Soetanto, Wei-Chih Wang, "A platform-based foot pressure/shear sensor", Proc. SPIE 8348, Health Monitoring of Structural and Biological Systems 2012, 83481U (20 April 2012); doi: 10.1117/12.915396;
9. Dumbleton T, Buis AW, McFayden A, McHugh BF, McKay G, Murray KD, et al. "Dynamic interface pressure distributions of two transtibial prosthetic socket concepts." J Rehabil Res Dev 2009;46(3):405–15.
10. Gere, J. M., & Goodno, B. J. (2018). Mechanics of Materials. Cengage Learning.
11. Gindy, S. "Further developments in strain gage tactile sensing" (Eaton Corp., Troy, MI, United States) Source: SENSORS '86, p MS86-941/1-17, 1986
12. Halloway GA, Daly CH, Kennedy D, Chimoskey J. "Effects of external pressure loading on human skin blood flow measured by <sup>133</sup>Xe clearance." J Appl Physiol 1976;40(4):597–600.
13. Huang, H. (Dept. of Mech. & Aerosp. Eng., Univ. of Texas Arlington, Arlington, TX, United States); Farahanipad, F.; Singh, A.K. "A stacked dual-frequency microstrip patch antenna for simultaneous shear and pressure displacement sensing". Source: IEEE Sensors Journal, v 17, n 24, p 8314-23, 15 Dec. 2017
14. Laszczak, P. et al. "A pressure and shear sensor system for stress measurement at lower limb residuum/socket interface" Medical Engineering and Physics , Volume 38 , Issue 7 , 695 – 700
15. Lee VSP, Solomonidis SE, Spence WD. "Stump-socket interface pressure as an aid to socket design in prostheses for trans-femoral amputees - a preliminary study". Proc Inst Mech Eng H 1997;211(2):167–80

16. Mak AFT, Zhang M, Boone DA. "State-of-the-art research in lower-limb prosthetic biomechanics-socket interface: a review." *J Rehabil Res Dev.* 2001;38(2):161-174.
17. Mohsin I. Tiwana, Stephen J. Redmond, Nigel H. Lovell, "A review of tactile sensing technologies with applications in biomedical engineering", *Sensors and Actuators A: Physical*, Volume 179, 2012, Pages 17-31, ISSN 0924-4247, <https://doi.org/10.1016/j.sna.2012.02.051>.
18. B. J. P. Mortimer, G. A. Zets, B. J. Altenbernd and T. Goonetilleke, "Development of a planar shear sensor," 2016 38th Annual International Conference of the IEEE Engineering in Medicine and Biology Society (EMBC), Orlando, FL, 2016, pp. 2030-2033. doi: 10.1109/EMBC.2016.7591125
19. Pohjolainen, T., Alaranta, H., & Wikstrom, J. (1989). Primary survival and prosthetic fitting of lower limb amputees. *Prosthetics and Orthotics International*, 13, 63-69. Retrieved from <http://journals.sagepub.com/doi/pdf/10.3109/03093648909078214>
20. Sanders, J. "Interface mechanics in external prosthetics: Review of interface stress measurement techniques". *Med. Biol. Eng. Comput.* 1995, 33, 509–516
21. Sanders, J., Daly, C. H., "Measurement of stresses in three orthogonal directions at the residual limb-prosthetic socket interface". *IEEE Transactions on Rehabilitation Engineering*, Vol 1, No 2, June 1993, 79-85
22. Sanders, J.E., Zachariah S.G., Jacobsen A.K., Ferguson J.R., "Changes in interface pressures and shear stresses over time on trans-tibial amputee subjects ambulating with prosthetic limbs: comparison of diurnal and six-month differences" *Journal of Biomechanics* , Volume 38 (2005) , Issue 8 , 1566 – 1573



23. Sewell, P., Noroozi, S., Vinney, J., & Andrews, S. (2000). Developments in the trans-tibial prosthetic socket fitting process: A review of past and present research. *Prosthetics and Orthotics International*, 24, 97-107. Retrieved from <http://journals.sagepub.com/doi/pdf/10.1080/03093640008726532>
24. Sundara-Rajan, K. (Dept. of Electr. Eng., Univ. of Washington, Seattle, WA, United States); Rowe, G.I.; Simon, A.J.; Klute, G.K.; Ledoux, W.R.; Mamishev, A.V. "Shear sensor for lower limb prosthetic applications" Source: 2009 First Annual ORNL Biomedical Science & Engineering Conference: Exploring the Intersections of Interdisciplinary Biomedical Research (BSEC 2009), p 4 pp., 2009
25. Tiwana, M.I., Shashank, A.; Redmond, S.J., Lovell, N.H. "Characterization of a capacitive tactile shear sensor for application in robotic and upper limb prostheses" Source: *Sensors and Actuators: A Physical*, v 165, n 2, p 164-72, Feb. 2011
26. Zhang M, Roberts VC. "The effect of shear forces externally applied to skin surface on underlying tissues". *J Biomed Eng* 1993;15(6):451-6.
27. Zhang M, Turner-Smith AR, Roberts VC, Tanner A. "Frictional action at lower limb/prosthetic socket interface". *Med Eng Phys* 1996;18(3):207-14.
28. Ziegler-Graham, Kathryn, et al. "Estimating the Prevalence of Limb Loss in the United States: 2005 to 2050". *Archives of Physical Medicine and Rehabilitation*, vol. 89, no. 3, 2008, pp. 422-429., doi:10.1016/j.apmr.2007.11.005.

## BIOGRAPHICAL INFORMATION

Elida Esmeralda Sorto-Ramos will be graduating with an Honors degree in Aerospace Engineering from the University of Texas at Arlington in May 2019. While at UTA she served Vice President of Freshman and Transfer Engineering Student Council and a member of the Society of Women Engineers and the American Institute of Aeronautics and Astronautics.

In her sophomore year she joined the research team at the Advanced Sensor Technology Laboratory under the direction of Dr. Haiying Huang where she assisted in the development of interfacial shear and pressure sensors for the optimization of prosthetic socket fitting. She has since participated in undergraduate research sponsored by the McNair Scholars program and a Research Experience for Undergraduates. Through the McNair Scholars program Elida had the opportunity to travel to professional conferences (AIAA Space 2018, AIAA SciTech 2019) and visit graduate schools.

In her last semester, Elida conducted research in the Aerospace Vehicle Design Laboratory, investigating the legacy of rocket propulsion systems. After graduation, Elida will attend graduate school at Stanford University where she will pursue her Masters and Doctoral degrees in Aerospace Vehicle Design. Elida's research interests include multidisciplinary design integration and analysis of space access vehicles.

Elida enjoys hiking, kayaking, and traveling, having already visited 20 countries.